1634 *Inorg. Chem.* **2010**, *49*, 1634–1646
DOI: 10.1021/ic9020299

Inorganic Chemistry
Article

Solvatochromic and Ionochromic Effects of Iron(II)bis-(1,10-phenanthroline)dicyano: a Theoretical Study

Ivelina Georgieva,*,† Adélia J. A. Aquino,‡ Natasha Trendafilova,† Paulo S. Santos,§ and Hans Lischka*,‡

†*Institute of General and Inorganic Chemistry, Bulgarian Academy of Sciences, Sofia, Bulgaria,* ‡*Institute for Theoretical Chemistry, University of Vienna, Vienna, Austria, and* §*Instituto de Química, Universidade de São Paulo, São Paulo, Brazil*

Received October 14, 2009

Solvatochromic and ionochromic effects of the iron(II)bis(1,10-phenanthroline)dicyano ($Fe(phen)_2(CN)_2$) complex were investigated by means of combined DFT/TDDFT calculations using the PBE and B3LYP functionals. Extended solvation models of $Fe(phen)_2(CN)_2$ in acetonitrile and aqueous solution, as well as including interaction with Mg^{2+}, were constructed. The calculated vertical excitation energies reproduce well the observed solvatochromism in acetonitrile and aqueous solutions, the ionochromism in acetonitrile in the presence of Mg^{2+}, and the absence of ionochromic effect in aqueous solution. The vertical excitation energies and the nature of the transitions were reliably predicted after inclusion of geometry relaxation upon aqueous micro- and global solvation and solvent polarization effect in the TDDFT calculations. The two intense UV−vis absorption bands occurring for all systems studied are interpreted as transitions from a hybrid Fe^{II}(d)/cyano N(p) orbital to a phenanthroline π^* orbital rather than a pure metal-to-ligand-charge transfer (MLCT). The solvatochromic and ionochromic blue band shifts of $Fe(phen)_2(CN)_2$ were explained with preferential stabilization of the highest occupied Fe^{II}(d)/cyano N(p) orbitals as a result of specific interactions with water solvent molecules or Mg^{2+} ions in solution. Such interactions occur through the CN^- groups in the complex, and they have a decisive role for the observed blue shifts of UV−vis absorption bands.

Introduction

The literature on solvatochromism is copious and demonstrates the ever increasing interest in the subject. The position of equilibrium, as well as reaction rates, are in general solvent dependent, and sometimes such dependency is dramatic, as is the case, for instance, of the molecular complex pyrene: cyclophane, whose formation constant changes by a factor of about one million when water is replaced by carbon disulfide.[1] Along the same lines, drastic changes in spectral transition energies have been observed for hundreds of substances.[2] The most comprehensive review on the subject is still the one due to C. Reichardt,[2] published in 1994, that is essentially focused on organic dyes, with just two mentions of metallic complexes, a tungsten carbonyl phenanthroline complex,[3] and an iron cyano phenanthroline species.[4] One aspect that draws attention in Reichardt's review is the scarce use of quantum chemical calculations to understand the molecular nature of the effect, and this is still true nowadays, mainly regarding the use of rigorous calculations and realistic models of solute−solvent interactions. Such interactions have been at the center of the chemist's interest for quite a long time, and nowadays a considerable effort is being dedicated to select suitable organic dyes to be used in the definition of operational scales of solvents, based mainly on spectral parameters. On the other hand, in the biological realm there are several biomolecules responsible for a myriad of biological functions that contain in their core a metallic center coordinated to organic moieties. In this respect, a more detailed understanding of the biomolecule-solvent interaction would be of extreme interest, and accordingly the use of species like $Fe(CN)_2(phen)_2$ as model systems for rigorous quantum chemical calculations seems to be the strategy of choice.

The presence of electronic transitions of different character (metal-to-ligand, metal-centered, ligand-to-ligand, intraligand, and ligand-to-metal) characterizes specific photophysical and photochemical properties of many transition metal complexes.[5] For certain classes of compounds these properties could be changed by the solvent environment or by the presence of metal ions in specific solution, producing solvatochromism and ionochromism, respectively. *cis*-Iron(II)-bis(1,10-phenanthroline)dicyano, $Fe(phen)_2(CN)_2$, exhibits

*To whom correspondence should be addressed. E-mail: ivelina@svr.igic.bas.bg (I.G.), hans.lischka@univie.ac.at (H.L.).

(1) Smithrud, D. B.; Diederich, F. J. *J. Am. Chem. Soc.* **1990**, *112*, 339–343.
(2) Reichardt, C. *Chem. Rev.* **1994**, *94*, 2319–2358.
(3) Kaim, W.; Olbrich-Deussner, B.; Roth, T. *Organometallics* **1991**, *10*, 410–415.
(4) Linert, W.; Gutman, V. *Coord. Chem. Rev.* **1992**, *117*, 159–183.
(5) Daniel, C. *Photochemistry of Transition Metal Complexes: Theory, Encyclopedia of Inorganic Chemistry*; John Wiley&Sons: New York, 2007.

 Published on Web 01/07/2010

significant solvatochromic and ionochromic band shifts in certain solutions.[6−8] Since such spectroscopic properties determine the sensor properties of this compound, they have been extensively studied using a variety of spectroscopic methods.[6] The UV−vis bands of $Fe(phen)_2(CN)_2$ have been used as an indicator of inorganic solvent polarity[9] as a Lewis acid−base indicator for estimation of the acceptor numbers of cations in aqueous and nonaqueous solutions[10] and as an indicator solute to monitor the effect of solute−solvent and solvent−solvent interactions on the preferential solvation characteristics.[11,12] $Fe(phen)_2(CN)_2$ absorption band shift has been applied also for assessment of the unknown acceptor numbers of binary solvent mixture[13] and to probe solvation in organized aqueous media such as micelles and microemulsions.[14] The absorption bands observed for $Fe(phen)_2(CN)_2$ in acetonitrile (at 597 and ∼520 nm) show negative solvatochromism, resulting in blue-shifts of the UV−vis bands in ethanol (at 560 and 490 nm) and in water (at 517 and 450 nm). The presence of Na^+, Li^+ and Mg^{2+} ions in acetonitrile produces also increasing negative ionochromism (blue-shifts of UV−vis bands, 562, 549, and 521 nm) with respect to the pure solvent. Interestingly, such a shift does not occur in aqueous solution.[6,7] The absorption bands of $Fe(phen)_2(CN)_2$ were interpreted in the literature as low-lying metal-to-ligand charge transfer transition (MLCT) from Fe^{II} (electron rich atom with a d^6 electron configuration) to phen (electron-acceptor ligand with low-lying π^* orbitals). For $[Fe(phen)_3]^{2+}$ and $[Fe(bpy)_3]^{2+}$ species, however, where cyano groups are missing, the solvatochromic effect is not observed.[15] Surface-enhanced Raman scattering (SERS) and surface-enhanced resonant Raman scattering (SERRS) data for $Fe(phen)_2(CN)_2$ predict strong interactions of the CN moiety with the acidic protons of the solvents and strong ion-pair interaction of cyano N with cations such as Li^+ and Mg^{2+}.[6] The role of CN^- and phen ligands as well as of the solvent environment for the solvatochromic and ionochromic band shifts of the iron(II) complex is far from being understood. Simulation and interpretation of absorption and emission spectra of the $Fe(phen)_2(CN)_2$ complex using quantum mechanical computations can provide a valuable aid to clarify the character of the transitions observed and to explain the solvatochromic and ionochromic shift.

In this work we study the spectroscopic and photophysical properties of the chromophore $Fe(phen)_2(CN)_2$ by means of combined density functional theory (DFT)/time dependent density functional theory (TDDFT) calculations using the B3LYP and PBE functionals. The DFT/Multireference configuration interaction (DFT/MRCI) method is applied for the calculations of vertical excitation energies of the $Fe(phen)_2(CN)_2$ complex. The results obtained are used as a reference to check the adequacy of the density functional methods. To gain deeper insight into the solvatochromic and ionochromic properties of $Fe(phen)_2(CN)_2$ from a theoretical point of view, realistic solvation models were developed and applied including specific solvent effects beyond the pure continuum approach, similar to our previous investigations on lanthanide complexes with coumarin-3-carboxylic acid.[16] It will be shown that for aqueous solution, consideration of the specific solvent interactions are crucial. The geometrical and electronic structure of $Fe(phen)_2(CN)_2$ and the properties of the Fe^{II}-phen/Fe^{II}−CN^- bonding are analyzed to find the specific parameters responsible for the observed band shifts in the UV−vis spectra in aqueous and acetonitrile solution, as well as in presence of Mg^{2+} in acetonitrile and the absence of ionochromic shift in aqueous solution.

Calculation Strategy. The band shifts for specific solvents were calculated on the basis of different model structures. The solvatochromic shift was investigated by using a global solvation model for the iron(II) complex in the non-protic solvent acetonitrile and a combined micro- and global solvation model for the complex in aqueous solution, Figure 1a, b. In the microsolvation model of $Fe(phen)_2(CN)_2$ the specific solute−solvent interactions are represented by means of clusters of four water molecules bonded to the CN^- groups of the iron(II) complex. The ionochromic study is performed by simulation of the solvent environment including metal ions. The clusters of $Fe(phen)_2(CN)_2$ with Mg^{2+}, $[Fe(phen)_2(CN)_2\cdots Mg]^{2+}$ and $[Fe(phen)_2(CN)_2\cdots 2Mg]^{4+}$, are investigated in acetonitrile, (Figure 1c, d) and in aqueous solution, $[Fe(phen)_2(CN)_2\cdots 2Mg(H_2O)_6]^{4+}$, $[Fe(phen)_2(CN)_2\cdots 2Mg(H_2O)_5]^{4+}$, and $[Fe(phen)_2(CN)_2\cdots Mg(H_2O)_6]^{2+}$, Figure 1e, f, g. The absorption spectra of the models studied are simulated by means of TDDFT calculations in the solvent, including solvent polarization effect on the vertical excitation energies.

Computational Details

The spin state calculations (^1A, ^3A, ^5A) and geometry optimization of $Fe(phen)_2(CN)_2$ were performed using different DFT functionals, nonhybrid PBE[17] and BP86[18] and the hybrid PBE0 (25%HF),[19,20] B3LYP (20%HF)[21,22] and BHLYP (50%HF).[21,23] The DFT[24] and HF[25] calculations were performed with the Turbomole program package.[26]

(6) Corio, P.; Temperini, M. L. A.; Rubin, J. C.; Santos, P. S. *Spectrochim. Acta A* **1999**, *55*, 2411–2421.
(7) (a) Burgess, J. *Spectrochim. Acta A* **1970**, *26*, 1369–1374. (b) Podsiadla, M.; Rzeszotarska, J.; Kalinowski, M. K. *Monatsh. Chem.* **1994**, *125*, 827−831 and references therein.
(8) Corio, P.; Temperini, M. L. A.; Santos, P. S. *Langmuir* **1999**, *15*, 2500–2507.
(9) Al-Aousy, A.; Burgess, J. *Inorg. Chim. Acta* **1990**, *169*, 167–170.
(10) Linert, W.; Jaeson, R. F.; Bauer, G.; Taha, A. *J. Coord. Chem.* **1997**, *42*, 211–229.
(11) (a) Burgess, J.; Morton, S. F. N. *J. Chem. Soc., Dalton Trans.* **1972**, 1712–1714. (b) Burgess, J.; Twigg, M. V. *J. Chem. Soc., Dalton Trans.* **1974**, 2032–2036.
(12) Taha, A.; Ramadan, A. A. T.; El-Behairy, M. A.; Ismail, A. I.; Mahmoud, M. M. *New J. Chem.* **2001**, *25*, 1306–1312.
(13) Taha, A.; Mahmoud, M. M. *New J. Chem.* **2002**, *26*, 953–957.
(14) Burgess, J.; Lane, R. C.; Singh, K.; de Castro, B.; Gameiro dos Santos, A. P. *J. Chem. Soc., Faraday Trans.* **1994**, *90*, 3071–3075.
(15) Pocker, Y.; Ciula, J. C. *J. Am. Chem. Soc.* **1989**, *111*, 4728–4735.
(16) Georgieva, I.; Trendafilova, N.; Aquino, A.; Lischka, H. *Inorg. Chem.* **2007**, *46*, 10926–10936.
(17) Perdew, J. P. R.; Burke, K.; Ernzerhof, M. *Phys. Rev. Lett.* **1996**, *77*, 3865–3868.
(18) Ahlrichs, R.; Furche, F.; Grimme, S. *Chem. Phys. Lett.* **2000**, *325*, 317–321.
(19) Adamo, C.; Barone, V. *J. Chem. Phys.* **1999**, *110*, 6158–6170.
(20) Perdew, J. P.; Ernzerhof, M.; Burke, K. *J. Chem. Phys.* **1996**, *105*, 9982–9985.
(21) Lee, C.; Yang, W.; Parr, R. G. *Phys. Rev B* **1988**, *37*, 785–789.
(22) Becke, A. D. *J. Chem. Phys.* **1993**, *98*, 5648–5652.
(23) Becke, A. D. *J. Chem. Phys.* **1993**, *98*, 1372–1377.
(24) (a) Treutler, O.; Ahlrichs, R. *J. Chem. Phys.* **1995**, *102*, 346–354. (b) Eichkorn, K.; Weigend, F.; Treutler, O.; Ahlrichs, R. *Theor. Chem. Acc.* **1997**, *97*, 119–124.
(25) Haser, M.; Ahlrichs, R. *J. Comput. Chem.* **1989**, *10*, 104–111.
(26) Ahlrichs, R.; Bär, M.; Häser, M.; Horn, H.; Kölmel, C. *Chem. Phys. Lett.* **1989**, *162*, 165–169.

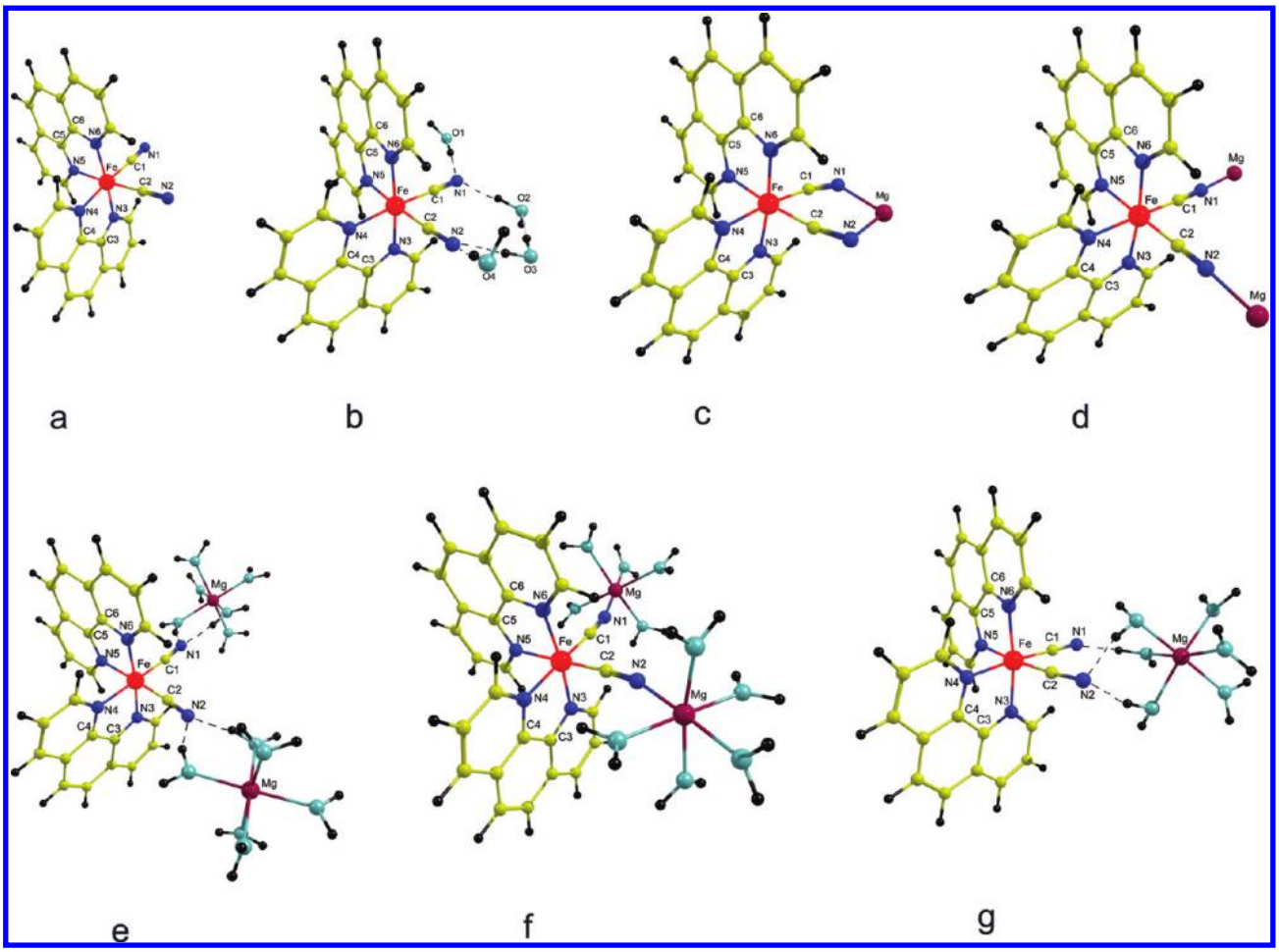

Figure 1. Model structures of (a) $Fe(phen)_2(CN)_2$ in acetonitrile, (b) microsolvated iron(II) complex in aqueous solution, $Fe(phen)_2(CN)_2\cdots 4(H_2O)$, (c) $[Fe(phen)_2(CN)_2\cdots Mg]^{2+}$ cluster in acetonitrile, (d) $[Fe(phen)_2(CN)_2\cdots 2Mg]^{4+}$ cluster in acetonitrile, (e) $[Fe(phen)_2(CN)_2\cdots 2(Mg(H_2O)_6)]^{4+}$ cluster in aqueous solution, (f) $[Fe(phen)_2(CN)_2\cdots 2(Mg(H_2O)_5)]^{4+}$ cluster in aqueous solution, and (g) $[Fe(phen)_2(CN)_2\cdots Mg(H_2O)_6]^{2+}$ cluster in aqueous solution.

A combination of different basis sets was applied for the ligand atoms and for the Fe atom with the purpose of finding a good compromise between efficiency and computational cost. The split-valence (SV(P))[27] basis set was used for initial calculations. To obtain a better description of the wave function in the ligand-Fe^{II} interaction region, additional diffuse functions were added (one s and one p set) for C1−C6 and N atoms (SV(P)+sp). This combined basis set is denoted as CB-1. The exponents of the diffuse functions were obtained by dividing the respective smallest exponent of the SV(P) basis set by a factor of 3, as described in previous investigations.[28] These diffuse functions were particularly important for the description of the negatively charged regions of the complexes. Moreover, it was found previously that the addition of these functions significantly reduces the basis set superposition error.[29] In addition, the TZVP[30] (17s11p6d)/[6s4p3d] and QZV[31] (24s18p10d)/[11s6p5d] basis sets were used on the Fe atom to test the effect of the basis set extension on Fe-ligand bond lengths.

For calculations of UV−vis absorption spectra, the 20 lowest singlet excited states of the closed shell complex in the gas phase were calculated by the TDDFT[32] method as implemented in the Turbomole program. In spite of difficulties of TDDFT in treating charge-transfer states properly[33] the TDDFT approach remains a computationally simple and efficient method able to treat practical problems in a reasonable time scale at low cost as compared to highly correlated ab initio methods.[34] TDDFT calculations have proven to be quite reliable in describing also the electronic spectra of complexes containing transition metals in solution.[35]

The combined density functional and multireference configuration interaction method (DFT/MRCI) of Grimme and Waletzke was used for single point vertical excitation energy calculations at the obtained DFT equilibrium geometries of phen and $Fe(phen)_2(CN)_2$.[36] All required integrals were computed by the Turbomole package using the BHLYP/SVP method. Fifteen roots were computed for $Fe(phen)_2(CN)_2$

(27) Schäfer, A.; Horn, H.; Ahlrichs, R. *J. Chem. Phys.* **1992**, *97*, 2571–2577.
(28) (a) Aquino, A. J. A.; Tunega, D.; Haberhauer, G.; Gerzabek, M.; Lischka, H. *Phys. Chem. Chem. Phys.* **2000**, *2*, 2845–2850. (b) Georgieva, I.; Trendafilova, N.; Aquino, A. J. A.; Lischka, H. *J. Phys. Chem. A* **2005**, *109*, 11860–11869.
(29) Aquino, A. J. A.; Tunega, D.; Haberhauer, G.; Gerzabek, M. H.; Lischka, H. *J. Phys. Chem. A* **2002**, *106*, 1862–1871.
(30) Schäfer, A.; Huber, Ch.; Ahlrichs, R. *J. Chem. Phys.* **1994**, *100*, 5829–5835.
(31) Weigend, F. *Phys. Chem. Chem. Phys.* **2006**, *8*, 1057–1065.
(32) Bauernschmitt, R.; Ahlrichs, R. *Chem. Phys. Lett.* **1996**, *256*, 454–464.
(33) Dreuw, A.; Weisman, J. L.; Head-Gordon, M. *J. Chem. Phys.* **2003**, *119*, 2943–2946.
(34) Daniel, C. *Coord. Chem. Rev.* **2003**, *238*, 143–166.
(35) Barone, V.; Fabrizi de Biani, F.; Ruiz, E.; Sieklucka, B. *J. Am. Chem. Soc.* **2001**, *123*, 10742–10743.
(36) Grimme, S.; Waletzke, M. *J. Chem. Phys.* **1999**, *111*, 5645–5655.

within C_1 symmetry. The DFT/MRCI calculations are performed with 15 non-frozen, highest occupied orbitals. The reference configurations used were constructed by single and double excitations involving four electrons in the two energetically highest occupied orbitals and the two lowest unoccupied orbitals. The two occupied orbitals show mostly Fe(d) character (including and N(p) contribution from the cyano groups), whereas the two unoccupied orbitals are of phen(π*) type. The DFT/MRCI approach including dynamic electron correlation (by DFT) and static correlation effects (by MRCI) was applied to judge the quality of the TDDFT results.

The solvent effect on the $Fe(phen)_2(CN)_2$ geometry was studied simulating (1) specific solute−solvent interaction by means of water cluster models (microsolvation) and (2) combined micro- and global solvation by water cluster calculations in continuum medium using the Conductor-like Screening Model (COSMO) (implemented in Turbomole), where the solute molecule forms a cavity within the dielectric continuum of permittivity ε representing the solvent.[37] COSMO calculations were performed with default options and non-optimized radii of 1.8135 Å for N, 1.9890 Å for C, 1.7784 Å for O, 1.4040 Å for H, and 2.2230 Å for Fe.

The solvent effects in excited states were evaluated by a nonequilibrium implementation of the polarizable conductor model (CPCM)[38,39] using the GAUSSIAN03 package.[40] The solute molecular cavity is defined using the default united atom topological parameters set. The solvent effect on the excited state properties of $Fe(phen)_2(CN)_2$ and its Mg^{2+} clusters were calculated at TDDFT/PBE and TDDFT/B3LYP levels of theory with a combined basis set called CB-2 (SVP for C1−C6, N, Fe, and Mg and SV for all other C and H atoms) for the ground state structures optimized in gas phase at PBE/CB-1 level. The smaller basis CB-2 was chosen for excited state calculations in solution because of computational cost. The Chemcraft program[41] was applied for visualization of calculated absorption spectra using Lorentzian broadening and bandwidth on half height of 50.

Full geometry optimizations of all molecular systems were carried out without symmetry constraint. Frequency calculations were performed, and the minima on the potential energy surfaces of the reported structures were characterized by the absence of negative eigenvalues in the Hessian matrix. The character of the molecular orbitals contributing to the most intense transition was analyzed by means of Mulliken and natural population analysis (NPA).[42]

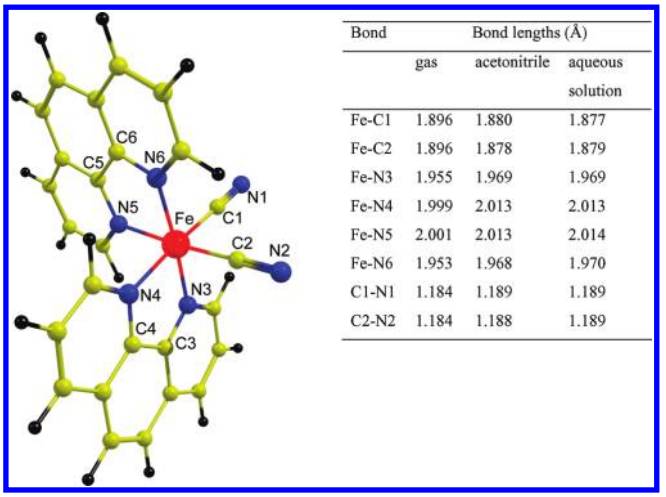

Bond	Bond lengths (Å)		
	gas	acetonitrile	aqueous solution
Fe-C1	1.896	1.880	1.877
Fe-C2	1.896	1.878	1.879
Fe-N3	1.955	1.969	1.969
Fe-N4	1.999	2.013	2.013
Fe-N5	2.001	2.013	2.014
Fe-N6	1.953	1.968	1.970
C1-N1	1.184	1.189	1.189
C2-N2	1.184	1.188	1.189

Figure 2. DFT/PBE/CB-1 geometry of $Fe(phen)_2(CN)_2$ in gas phase, acetonitrile, and aqueous solution.

The $Fe^{II}-CN^-$ and Fe^{II}-phen bonding situations for $Fe(phen)_2(CN)_2$ in gas phase, solution, and in the presence of Mg^{2+} ions were investigated in terms of the charge decomposition analysis (CDA).[43] The CDA decomposes the Kohn−Sham determinant of a complex [ML] in terms of fragment orbitals of the chosen ligand [L] and the metal [M]. The CDA calculations of the Fe^{II} complexes were performed at B3LYP/6-31G(d) level.

Results and Discussion

$Fe(phen)_2(CN)_2$ Complex in Vacuo. The *cis*-iron(II)-bis(1,10-phenanthroline)dicyano complex was modeled following the experimentally based suggestion[44] that the CN^- ligands are bound to Fe^{II} through the C atom (Figure 2). The DFT method with PBE, BP86, PBE0, B3LYP, and BHLYP functionals and HF method were applied to calculate the three possible spin states of the $Fe(phen)_2(CN)_2$ complex: singlet (^{1}A) (restricted), triplet (^{3}A), and quintet (^{5}A). The relative energies of the studied species are presented in the Supporting Information, Table S1. For the DFT functionals used in this work the restricted singlet state of $Fe(phen)_2(CN)_2$ is obtained as the most stable one. This finding is in good agreement with the fact that the magnetic susceptibility measurements show the $Fe(phen)_2(CN)_2$ complex to be diamagnetic.[12] Only the HF and BHLYP calculations show the quintet as the most stable state of $Fe(phen)_2(CN)_2$. In the HF approximation the Coulomb hole is completely neglected and thus the open shell stabilization (high spin states - ^{3}A, ^{5}A) is overestimated. As it is seen from the Supporting Information, Table S1, with decrease of the amount of HF-exchange in the order of HF, BHLYP, B3LYP, and PBE levels, the high spin state is destabilized. All calculations throughout this paper were performed for the singlet state (closed shell) of the $Fe(phen)_2(CN)_2$ complex.

To achieve correct absorption spectra calculations of the complex, DFT methods were tested as to geometry

(37) Klamt, A.; Schüürmann, G. *J. Chem. Soc., Perkin Trans.* **1993**, *2*, 799–805.
(38) Barone, V.; Cossi, M. *J. Phys. Chem. A* **1998**, *102*, 1995–2001.
(39) Cossi, M.; Rega, N.; Scalmani, G.; Barone, V. *J. Comput. Chem.* **2003**, *24*, 669–681.
(40) Frisch, M. J.; Trucks, G. W.; Schlegel, H. B.; Scuseria, G. E.; Robb, M. A.; Cheeseman, J. R.; Montgomery, Jr., J. A.; Vreven, T.; Kudin, K. N.; Burant, J. C.; Millam, J. M.; Iyengar, S. S.; Tomasi, J.; Barone, V.; Mennucci, B.; Cossi, M.; Scalmani, G.; Rega, N.; Petersson, G. A.; Nakatsuji, H.; Hada, M.; Ehara, M.; Toyota, K.; Fukuda, R.; Hasegawa, J.; Ishida, M.; Nakajima, T.; Honda, Y.; Kitao, O.; Nakai, H.; Klene, M.; Li, X.; Knox, J. E.; Hratchian, H. P.; Cross, J. B.; Bakken, V.; Adamo, C.; Jaramillo, J.; Gomperts, R.; Stratmann, R. E.; Yazyev, O.; Austin, A. J.; Cammi, R.; Pomelli, C.; Ochterski, J. W.; Ayala, P. Y.; Morokuma, K.; Voth, G. A.; Salvador, P.; Dannenberg, J. J.; Zakrzewski, V. G.; Dapprich, S.; Daniels, A. D.; Strain, M. C.; Farkas, O.; Malick, D. K.; Rabuck, A. D.; Raghavachari, K.; Foresman, J. B.; Ortiz, J. V.; Cui, Q.; Baboul, A. G.; Clifford, S.; Cioslowski, J.; Stefanov, B. B.; Liu, G.; Liashenko, A.; Piskorz, P.; Komaromi, I.; Martin, R. L.; Fox, D. J.; Keith, T.; Al-Laham, M. A.; Peng, C. Y.; Nanayakkara, A.; Challacombe, M.; Gill, P. M. W.; Johnson, B.; Chen, W.; Wong, M. W.; Gonzalez, C.; and Pople, J. A. *Gaussian 03*, Revision D.01; Gaussian, Inc.: Wallingford, CT, 2004.
(41) http://www.chemcraftprog.com/.
(42) Reed, A. E.; Curtiss, L. A.; Weinhold, F. *Chem. Rev.* **1988**, *88*, 899–926.
(43) (a) Dapprich, S.; Frenking, G. *J. Phys. Chem.* **1995**, *99*, 9352–9362. (b) Frenking, G.; Pidun, U. *J. Chem. Soc., Dalton Trans.* **1997**, 1653–1662. (c) The CDA calculations were carried out with the program CDA: Dapprich, S.; Frenking, G. *CDA*; Phillips-Universität: Marburg, 1994.
(44) Zhan, S.; Meng, Q.; You, G.; Wang, P.; Zheng, P. *Polyhedron* **1996**, *15*, 2655–2658.

Table 1. Calculated Vertical Excitation Energies (vex, in eV) and Oscillator Strengths for the Singlet Excitations of phen and $Fe(phen)_2(CN)_2$ in Vacuo[a]

phen						$Fe(phen)_2(CN)_2$					
B3LYP/SVP		PBE/SVP		DFT/MRCI/SVP		B3LYP/CB-1		PBE/CB-1		DFT/MRCI/SVP	
vex	osc.str	vex	osc.str	vex	osc.str	vex	osc. str	vex	osc.str	Vex	osc.str
4.03	0.000	3.71	0.001	3.76	0.000	1.79	0.004	1.26	0.006	1.93	0.001
4.24	0.068	3.92	0.048	4.47	0.048	1.80	0.006	1.31	0.000	**2.08**	**0.057**
4.74	0.086	4.27	0.049	**4.73**	**0.372**	1.98	0.001	1.32	0.003	**2.21**	**0.063**
				4.68^{exp}							
5.05	**0.642**	**4.73**	**0.479**	4.89	0.065	1.99	0.008	1.35	0.001	2.27	0.010
5.46	0.098	4.89	0.044	5.44	0.137	2.02	0.001	1.44	0.000	2.28	0.001
5.61	**0.303**	5.16	0.001	**5.49**	**0.820**	2.07	0.006	1.49	0.002	2.31	0.004
				5.46^{exp}							
5.82	0.005	**5.17**	**0.083**	5.81	0.026	**2.16**	**0.052**	1.50	0.001	2.38	0.050
5.99	0.033	5.41	0.002	5.88	0.011	2.26	0.008	1.57	0.001	2.45	0.002
6.08	0.227	5.52	0.454	6.11	0.095	**2.27**	**0.058**	1.62	0.001	2.56	0.028
6.24	0.104	5.82	0.139	6.18	0.061	2.31	0.003	1.63	0.001	2.58	0.009
						2.39	0.024	**1.82**	**0.122**	2.62	0.027
						2.56	0.014	**2.10**	**0.022**		

[a] The two excitation energies with large oscillator strengths are given in bold. *exp*− experimental band maxima at eV ref. (48)

parameters and vertical excitation energies.[5] DFT geometry optimizations were performed for $Fe(phen)_2(CN)_2$ with various functionals and basis sets, and selected geometrical parameters are compared with available X-ray structural data.[44] The defined basis sets and the geometry parameters are presented in the Supporting Information, Table S2. A survey of the calculated geometry data indicates that the best agreement with experimental Fe^{II}−C and Fe^{II}−N bond lengths[44] is obtained at the PBE level and therefore it is used for geometry optimizations of $Fe(phen)_2(CN)_2$ and its Mg^{2+} clusters in gas phase and solution. Additionally, increasing the basis set for Fe^{II} (SVP, TZVP, QZV) and for C, N, H atoms (SV(P), TZVP) resulted in almost no changes in the Fe^{II}-ligand bond lengths (up to 0.004 Å). To get a good compromise between efficiency and computational costs the basis set CB-1 is used. The CB-1 basis set contains a SV(P)+sp basis for C1−C6 and N atoms and SV(P) basis for the C, H, Fe, and Mg atoms.

Vertical Excitations of Singlet Excited States of Fe(phen)$_2$(CN)$_2$. The vertical excitation energies of the singlet excited states of $Fe(phen)_2(CN)_2$ (PBE/CB-1 geometry) and the oscillator strengths were calculated with PBE, PBE0, B3LYP, BHLYP functionals and the CB-1 basis set. The calculated absorption spectra reveal two intense bands and the corresponding transition energies increase in the following order: PBE (1.82/2.10 eV) < B3LYP (2.16/2.27 eV) < PBE0 (2.33/2.44 eV) < BHLYP (3.37/3.44 eV). As discussed previously[45,46] the choice of the functional has a significant influence on the TDDFT transition energies. The transition energies mentioned above increase with increase of the amount of HF exchange in the functional. Similar effects have been observed for ruthenium[45] and copper complexes.[47] In general, the energies of the HOMO were predicted to be too high by the GGA approaches such as PBE (0% HF). The introduction of some HF exchange (as B3LYP - 20% HF) significantly decreases the degree of delocalization and stabilizes the highest occupied molecular orbital (HOMO). At the same time, the lowest unoccupied orbital (LUMO) is destabilized. As a result B3LYP transition energies become larger as compared to those of PBE. Reference data for vertical excitation energies of phen and $Fe(phen)_2(CN)_2$ based on the combined DFT/MRCI method (see Computational Methods) are presented in Table 1. The DFT/MRCI vertical excitation energies of phen (4.73, 5.49 eV) reproduce well the values of the experimental band maxima (4.68, 5.46 eV) in aqueous solution.[48] In comparison to DFT/MRCI calculations, B3LYP singlet excitation energies of phen show larger values up to ~0.2 eV, whereas those with the PBE functional reveal smaller values up to ~0.3 eV. The TDDFT/B3LYP and TDDFT/PBE excitation energies of $Fe(phen)_2(CN)_2$ are in good agreement with the DFT/MRCI results. The B3LYP excitation energies of 2.16/2.27 eV are close to the DFT/MRCI values of 2.08/2.21 eV, whereas the PBE excitation energies are lower (1.82/2.10 eV). Hence, the TDDFT/B3LYP method appears to be quite reliable for the prediction of the vertical excitation energies of $Fe(phen)_2(CN)_2$.

The vertical excitation calculations with the CB-1 basis set in aqueous and acetonitrile solution are very time-consuming. Therefore, the reduced basis set CB-2 was used further in the TDDFT calculations, both in gas phase and in solution. The results obtained with the CB-2 basis set were in good agreement with those obtained with CB-1.

Both B3LYP and PBE calculations predict MLCT character for all the excitations studied in this work. This assignment is confirmed by DFT/MRCI calculations. In particular, according to Mulliken and natural population analyses the excitations related to the large oscillator strength have multitransition character and involve transitions from dominant Fe(d) orbitals, which is in a

(45) (a) Ben Amor, N; Záliš, S.; Daniel, C. *Int. J. Quantum Chem.* **2006**, *106*, 2458–2469. (b) Záliš, S.; Ben Amor, N.; Daniel, C. *Inorg. Chem.* **2004**, *43*, 7978–7985. (c) Dreuw, A.; Head-Gordon, M. *J. Am. Chem. Soc.* **2004**, *126*, 4007–4016.

(46) (a) Casida, M. N.; Salahub, D. R. *J. Chem. Phys.* **2000**, *113*, 8918–8935. (b) Tozer, D. J. *J. Chem. Phys.* **2000**, *112*, 3507–3515.

(47) Szilagyi, R. K.; Metz, M.; Solomon, E. I. *J. Phys. Chem. A* **2002**, *106*, 2994–3007.

(48) (a) Krumholz, P. *J. Am. Chem. Soc.* **1951**, *73*, 3487–3492. (b) Yamasaki, K.; Hara, T.; Yasuda, M. Proceedings of the Japan Academy, 1953; Vol. *29*, p 337.

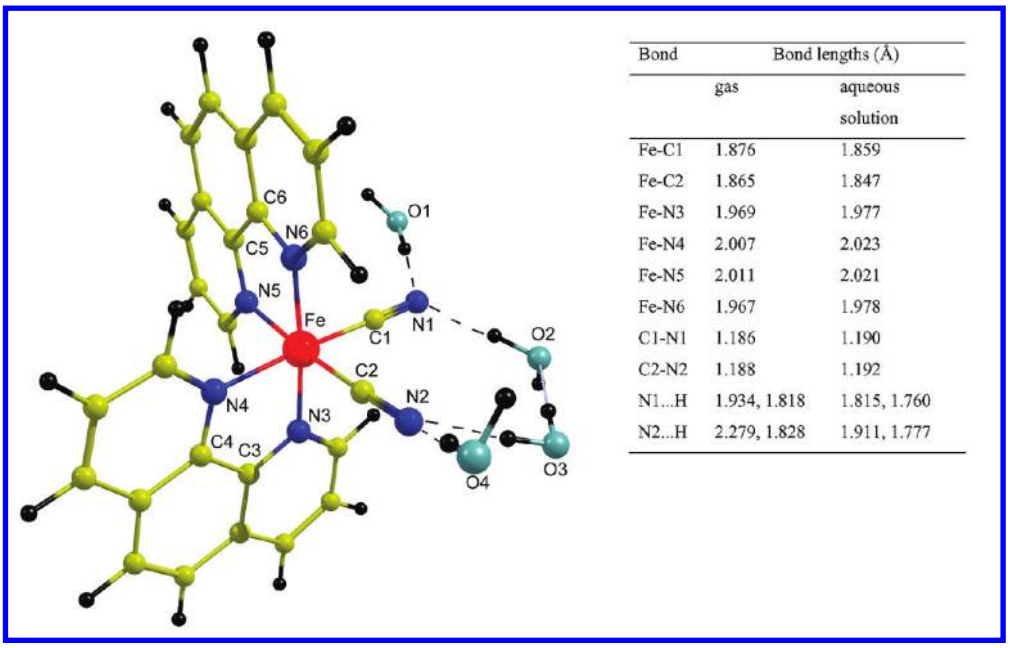

Bond	Bond lengths (Å)	
	gas	aqueous solution
Fe-C1	1.876	1.859
Fe-C2	1.865	1.847
Fe-N3	1.969	1.977
Fe-N4	2.007	2.023
Fe-N5	2.011	2.021
Fe-N6	1.967	1.978
C1-N1	1.186	1.190
C2-N2	1.188	1.192
N1...H	1.934, 1.818	1.815, 1.760
N2...H	2.279, 1.828	1.911, 1.777

Figure 3. DFT/PBE/CB-1 geometry of $Fe(phen)_2(CN)_2\cdots4(H_2O)$ complex in gas phase (microsolvation) and in aqueous solution (micro+global solvation).

non-bonding combination with the cyano N(p) orbitals (HOMO, HOMO-1, HOMO-2) to phen(π^*) orbitals (LUMO, LUMO+1, LUMO+2, LUMO+3).

Solvatochromism: $Fe(phen)_2(CN)_2$ in Solution. To simulate the absorption band shifts of $Fe(phen)_2(CN)_2$ in aqueous solution relative to acetonitrile, a series of quantum mechanical calculations were performed in both solvents. The $Fe(phen)_2(CN)_2$ geometry was optimized in acetonitrile and in aqueous solution using COSMO (global solvation), Figure 2. In addition, the geometry optimization of the Fe^{II} complex is performed simulating aqueous microsolvation by means of the $Fe(phen)_2(CN)_2\cdots4(H_2O)$ cluster and concomitant global aqueous solvation, Figure 3.

As can be seen from Figure 2, in acetonitrile and in aqueous global solution the Fe−C bond lengths are shortened by ~0.017 Å, whereas all Fe−N bond lengths are elongated by ~0.014 Å as compared to the gas phase geometry. The global water solvation (ε = 78.39) and the global solvation in acetonitrile (ε = 36.64) produce similar bond lengths of the complex. Specific water interactions are required (combined micro- and global aqueous solvation) to obtain a reliable differentiation between the effects of the two solvents. As a result, the Fe−C bond lengths shorten by ~0.027 Å and the Fe−N bond lengths elongate by ~0.01 Å in aqueous solution, Figure 3. As it will be shown below, this point appears to be crucial for simulation of the observed solvatochromic band shift also.

The TDDFT/B3LYP/CB-2 absorption spectra in gas phase, acetonitrile, and aqueous solution for $Fe(phen)_2(CN)_2$ optimized at PBE/CB-1 level in the corresponding environment, along with the orbitals which contribute to the most intense transition (pointed with a green arrow) are shown in Figure 4. Considering the most intense transition, the B3LYP vertical excitation energy in vacuo (2.19 eV (567 nm)) increases in acetonitrile (2.59 eV (480 nm)). The calculated excitation energy in aqueous solution (micro- and global solvated $Fe(phen)_2(CN)_2$) was found to be higher (2.98 eV (417 nm) as compared to acetonitrile. The obtained higher energy shift for the most intense absorption band going from acetonitrile to aqueous solution is in good agreement with the experimental blue band shift (2.08 eV (597 nm) (acetonitrile) → 2.40 eV (517 nm) (water)).[6] If only the continuum model was applied the vertical excitations in acetonitrile and aqueous solution were practically identical (2.59 eV, 2.63 eV) showing again the necessity to include specific solvation effects in the case of water.

In summary, the TDDFT/B3LYP calculations reproduce well the direction and the value of the solvent shift of the most intense band (Δ_{B3LYP} = 0.39 eV, Δ_{exp} = 0.32 eV). The B3LYP calculations produce larger vertical excitation energies (absolute values) by ~0.5 eV than the experimental band maxima. For comparison, the absorption spectra calculated at the TDDFT/PBE/CB-2 level are given in Figure 5. A higher energy band with low intensity along the most intense absorption band is observed and hence, the calculated spectra reproduce well the experimental absorption band shapes.[6] TDDFT/PBE calculations reproduce the blue shift of the two absorption bands going from acetonitrile (637 nm (1.94 eV), 553 nm (2.24 eV)) to aqueous solution (601 nm (2.06 eV), 527 nm (2.35 eV)). The solvent shift value (Δ_{PBE} = 0.11 eV), however, is smaller as compared to the experimental one. TDDFT/PBE level calculates lower vertical excitation energies (absolute value) by ~0.1−0.4 eV. The orbital plots shown for B3LYP (Figure 4) and PBE (Figure 5) reveal the same MLCT character of the solvatochromic bands of $Fe(phen)_2(CN)_2$ in acetonitrile and aqueous solutions as it was found for the most intense transition in vacuo.

To gain deeper insight into the band shifts going from gas phase to aqueous solution, two contributions are considered: the polarization induced by the solvent and the geometry relaxation changes from gas phase to polar

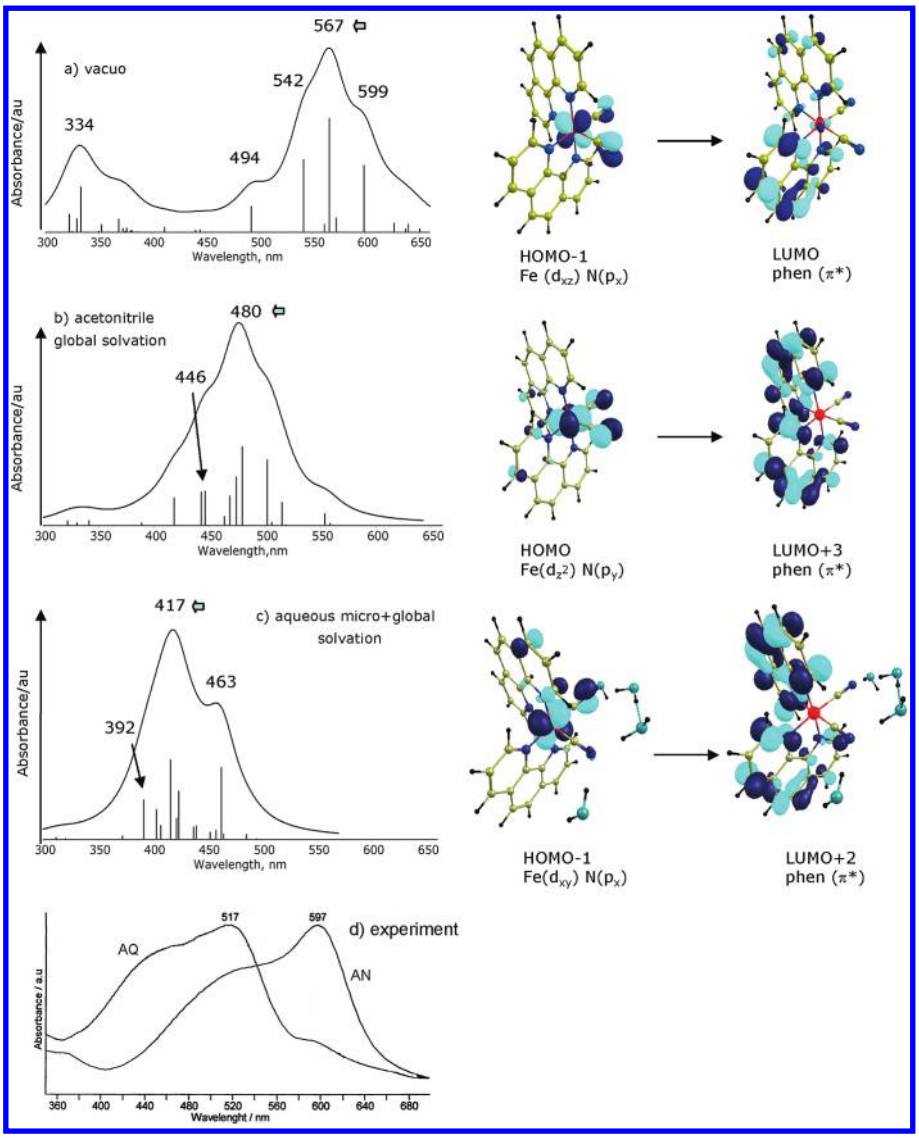

Figure 4. TDDFT/B3LYP/CB-2 absorption spectra of $Fe(phen)_2(CN)_2$ in (a) vacuo, (b) acetonitrile, (c) aqueous solution (micro + global solvation), and (d) comparison with the experimental absorption spectra.[6] Plots of orbitals contributing to the most intense transition.

aqueous solvent. Figure S1 (in Supporting Information) shows the energy scheme of calculated transition energies in gas phase and aqueous solution for the aqueous micro- and global solvated $Fe(phen)_2(CN)_2$ complex. The solvent effect computed on the basis of the globally hydrated $Fe(phen)_2(CN)_2\cdots4(H_2O)$ complex amounts to 0.6 eV (gas phase 2.38 eV vs aqueous solution 2.98 eV). The geometry relaxation effect is evaluated to be 0.2 eV by comparison of the calculated electronic excitations (with the largest oscillator strength) in gas phase for $Fe(phen)_2(CN)_2$ (2.19 eV) and hydrated $Fe(phen)_2(CN)_2\cdots4H_2O$ (2.38 eV). Hence, the solvent polarization produces in aqueous solution a larger increase of the excitation energy as compared to the energy increase upon geometry relaxation. Obviously, both the geometry relaxation and the solvent polarization effect lead to higher energy solvent shift, the last one being dominant. This can be understood by looking at the nature of the transitions: in all cases the absorption band maxima are due to a Fe(d)/cyanoN(p) → phen(π*) transition. Our calculations show that the mixed Fe(d)/cyanoN(p) orbital is non-bonding and, consequently, the energy of this orbital is slightly affected by changes in the bond distances, while it is strongly affected by interaction with the solvent. The effect of the acetonitrile and aqueous solvents on the orbitals is presented in Figure S2 (in Supporting Information). The HOMO, HOMO-1, HOMO-2 with Fe(d)/cyano N(p) contributions and LUMO, LUMO+1, LUMO+2, LUMO+3 with phen(π*) contributions are considered, all included in the MLCT of absorption band maxima. The energies of both Fe(d)/cyano N(p) and phen(π*) orbitals are lowered in solution, but the Fe(d)/cyanoN(p) orbitals are more stabilized than the phen(π*) orbitals, causing the calculated higher energy transition (gas phase → solution). The present calculations showed that the specific solute-aqueous solvent interactions (microsolvation) produce an additional stabilization of the HOMOs, causing higher transition energies, that is, the solvatochromic blue band shift (acetonitrile → aqueous solution). Obviously, the Fe(d)/cyanoN(p) orbitals are sensitive to hydrogen bonding of water molecules, and the specific interactions lead to a preferential stabilization of the Fe(d)/cyanoN(p) orbitals. The interaction of the water molecules with the $Fe(phen)_2(CN)_2$ complex occurs

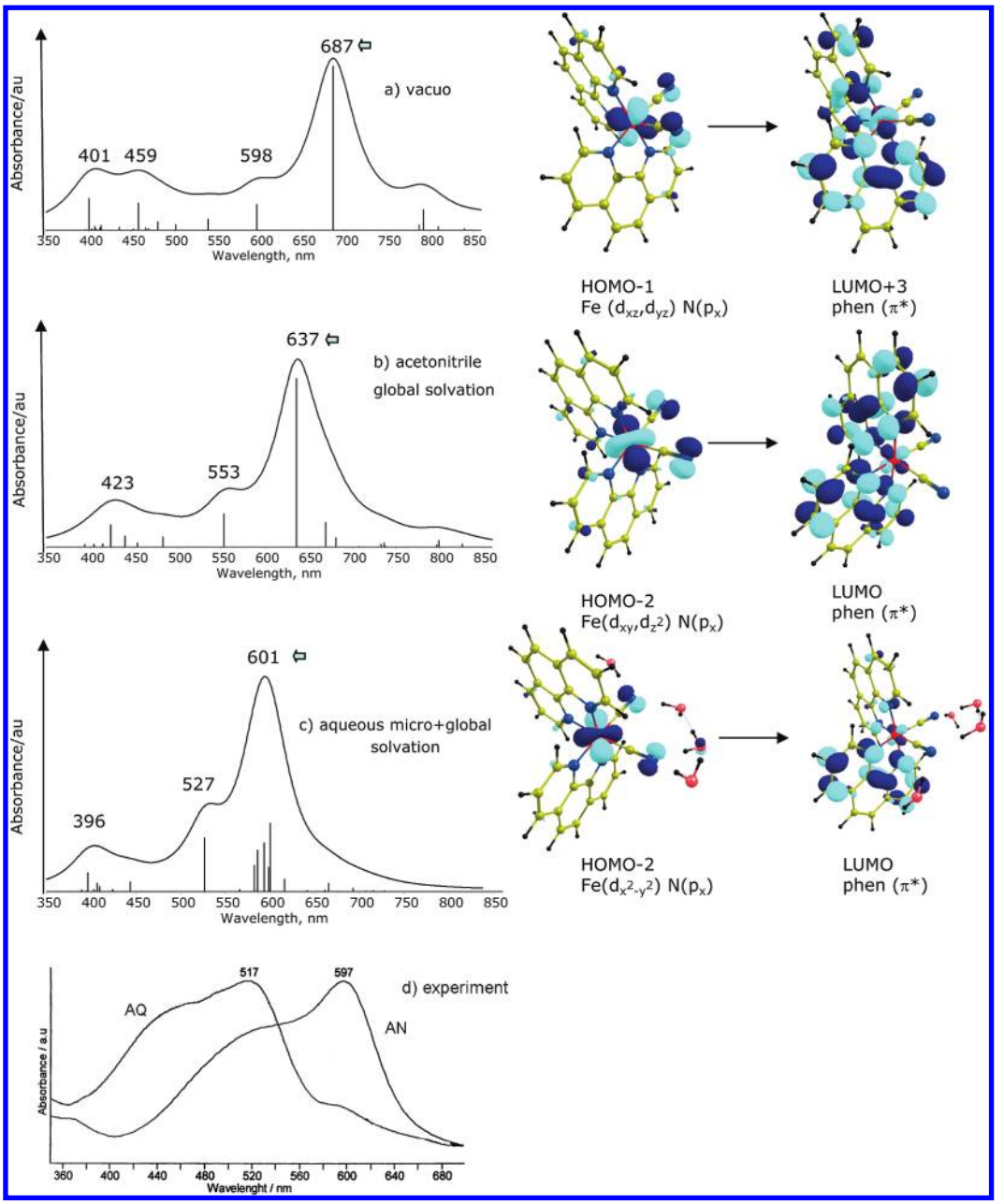

Figure 5. TDDFT/PBE/CB-2 absorption spectra of $Fe(phen)_2(CN)_2$ in (a) vacuo, (b) acetonitrile, (c) aqueous solution (micro + global solvation), and (d) comparison with the experimental absorption spectra.[6] Plots of orbitals contributing to the most intense transition.

primarily with the electronic charge on the nitrogen atoms of the CN^- groups, which appears to be an important factor for the observed blue band shift in aqueous solution.

The change in the dipole moment is another useful characteristic which could give insight into the origin of the blue shift in the UV−vis bands of the Fe^{II} complex between acetonitrile and aqueous solution. The dipole moment of $Fe(phen)_2(CN)_2$ (13.3 D in gas phase) increases to 22.8 D because of microsolvation and to 29.0 D when micro- and global aqueous solvation is applied. The dipole moment of 29.0 D in aqueous solution is even significantly larger as compared to that in the non-protic acetonitrile solvent (20.5 D), reflecting the more effective charge-separation favored in water. Fantacci et al. have shown that the transfer of electronic charge from metal(d) to ligand(π^*) produces a reduction of the dipole moment in the excited state and, as a consequence, the excited state is less stabilized by polar solvents than the ground state.[49] Hence, the larger dipole in aqueous solution than that in acetonitrile, which is in parallel to the larger ground state stabilization, correlates well with the observed blue UV−vis shift in the solvents studied. Obviously, ground state stabilization of $Fe(phen)_2(CN)_2$ in aqueous solution mainly contributes to the observed solvatochromic band shift. The increasing dipole moment in aqueous solution is due to the specific solute−solvent interactions. In the case of global acetonitrile and aqueous solutions, the calculated dipole moments are similar (20.5 D, 20.8 D).

(49) Fantacci, S.; De Angelis, F.; Selloni, A. *J. Am. Chem. Soc.* **2003**, *125*, 4381–4387.

Table 2. Charge Decomposition Analysis (CDA) of the $Fe(phen)_2(CN)_2$ System at DFT/B3LYP/6-31G(d) Level[a]

	CDA					
	q[d]		*q*[b]		*q*[r]	
system	Fe-CN	Fe-phen	Fe-CN	Fe-phen	Fe-CN	Fe-phen
$Fe(phen)_2(CN)_2$	0.635	0.418	0.118	0.224	−0.331	−0.502
$Fe(phen)_2(CN)_2\cdots4(H_2O)$	0.707	0.414	0.264	0.281	−0.395	−0.468
$[Fe(phen)_2(CN)_2\cdots2Mg]^{4+}$	0.420	0.477	0.230	0.138	−0.295	−0.357

[a] q is electronic charge in e. *q*[d] Donation $L\rightarrow Fe^{II}$. *q*[b] Back-donation $Fe^{II}\rightarrow L$. *q*[r] Repulsive polarization r. The non-classical rest term Δ was in all cases virtually zero (absolute values).

The induced polarization along the N←C←Fe bonding, caused by water interactions with the nitrogen cyano groups of the Fe^{II} complex coincides with the dipole moment direction of the complex, and thus it also strengthens the dipole moment in aqueous solution. The natural charges of cyano nitrogens become more negative in aqueous solution as compared to acetonitrile.

Because of the sensitivity of the Fe(d)/cyanoN(p) orbital energy to the solvent and its important role for solvatochromic band shift of $Fe(phen)_2(CN)_2$, we performed a Charge Decomposition Analysis (CDA) of the bonding properties of the $Fe^{II}-CN^-$ and Fe^{II}-phen and of the electron density of Fe in gas phase and in the case of specific water solvent interactions. The three components of the linear combination of the donor and acceptor fragment orbitals (LCFO) wave function of the complexes are calculated (Table 2): (i) the charge donation *d* given by the mixing of the occupied orbitals of the donor and the unoccupied orbitals of the acceptor; (ii) the back-donation *b* given by mixing of the occupied orbitals of the acceptor and the unoccupied orbitals of the donor; (iii) the charge depletion of the overlapping area (charge polarization) *r* given by the mixing of donor and acceptor; the nonclassical rest term Δ resulting from the mixing of unoccupied orbitals on the two fragments is close to the virtually zero as it is expected in a donor−acceptor complex.[43] The Fe-CN^- bonding situation is analyzed using the $[Fe(phen)_2CN]^+$ and CN^- fragments. The analysis of the Fe-phen bond uses $Fe(phen)(CN)_2$ and phen as bonding partners. An analogous fragment analysis is performed for the microhydrated complex $Fe(phen)_2(CN)_2\cdots4(H_2O)$. The CDA calculations predict $L\rightarrow M$ σ-donation and $M\rightarrow L$ π-back-donation contributions to the $Fe^{II}-CN^-$ and Fe^{II}-phen bonds, and the former is dominant. Indication for π-back-donation contribution to the Fe^{II}-phen and $Fe^{II}-CN^-$ bonding was given also from the trend of $Fe^{II}-C/N$ bond lengths elongation with increase of the HF exact exchange from PBE (0%HF) up to BHLYP (50% HF), Supporting Information, Table S2. A similar correlation of M−L bonds with the amount of HF exchange in the density functionals was already reported for the systems with significant π-back-donation M−L bonding, whereas this trend is opposite for the systems with mainly donation and electrostatic M−L bonding.[16,50,51] Upon introduction of water interactions, the σ-donation and the π-back-donation to the $Fe^{II}-CN^-$ bond increase (especially the latter contribution) whereas the contributions to the Fe^{II}-phen bonds change only slightly, Table 2. The trends found are in line with the decrease of the Fe−C bond lengths upon micro- and global solvation, Figures 2 and 3. The increased π-back-donation contribution to the $Fe^{II}-CN^-$ bond in aqueous solution leads to a lowering of the electron density on the transition metal. At the same time the Fe(d)/cyano N(p) orbital, contributing to the most intense transition is stabilized in aqueous solution, causing higher energy transition and blue band shift.

Ionochromism: $Fe(phen)_2(CN)_2$ in the Presence of Mg^{2+} in Solution. In the presence of metal cations like Mg^{2+} in acetonitrile solution, the $Fe(phen)_2(CN)_2$ complex exhibits ionochromism (absorption band blue-shifted by ∼80 nm).[6] The blue shifts of two absorption bands, the most intense one at 597 nm → 521 nm and low intense one at 520 nm → 460 nm are observed in the UV−vis spectrum. In aqueous solution, however, an ionochromic effect is not observed. For better understanding of the origin of the ionochromism, clusters of $Fe(phen)_2(CN)_2$ and Mg^{2+} in acetonitrile and aqueous solutions were investigated, Figure 1c−g. In these models the interaction of $Fe(phen)_2(CN)_2$ with Mg^{2+} occurs through the cyano nitrogen atoms. In acetonitrile two clusters with one and two Mg^{2+} ions were computed (Figure 1c, d). The Mg^{2+} ions have direct contact with the nitrogen atom of the cyano groups. In aqueous solution two hydrated Mg^{2+} ions are connected either directly to the cyano N atoms (Figure 1f) or one and two hydrated Mg^{2+} ions interact with the cyano N through water bridges of their hydration shell (Figure 1e, g). To predict the most stable structure of Mg^{2+} clusters of $Fe(phen)_2(CN)_2$ in acetonitrile and in aqueous solution, the formation energies were calculated using the reaction equations given in Table 3. According to these data, the $[Fe(phen)_2(CN)_2\cdots2Mg]^{4+}$ structure (Figure 6) is about twice as stable in acetonitrile than the complex $[Fe(phen)_2(CN)_2\cdots Mg]^{2+}$ containing one magnesium cation. The $[Fe(phen)_2(CN)_2\cdots2Mg(H_2O)_6]^{4+}$ structure (the Mg^{2+} is bonded to cyano N atom through two hydrated molecules) is the preferred one in aqueous solution (Figure 7) in comparison with the directly bonded hydrated Mg^{2+}. In case of Mg^{2+} clusters, the inclusion of the solvent effects in the TDDFT computations has a large effect on the transition energies leading to spectra in agreement with the experimental ones.

Selected bond lengths (at PBE/CB-1 level) in gas phase and in solution are given for the most stable structures, $[Fe(phen)_2(CN)_2\cdots2Mg]^{4+}$ and $[Fe(phen)_2(CN)_2\cdots2Mg(H_2O)_6]^{4+}$, in Figures 6, 7. The bond lengths of the other clusters are shown in Supporting Information, Figures S3,

(50) (a) Lamsabhi, A. M.; Alcamí, M. T.; Mo, O.; Yánez, M.; Tortajada, J. *ChemPhysChem* **2004**, *5*, 1871–1878. (b) Noguera, M.; Sodupe, M.; Bertrán, J. *J. Phys. Chem. A* **2004**, *108*, 333–341.

(51) Georgieva, I.; Trendafilova, N.; Rodriguez Santiago, L.; Sodupe, M. *J. Phys. Chem. A* **2005**, *109*, 5668–5676.

Table 3. DFT/PBE/CB-1 Formation Energies ΔE_f (kcal/mol) of the Mg^{2+} Clusters of $Fe(phen)_2(CN)_2$ in Acetonitrile (AN) and Aqueous (aq) Solution

reaction	ΔE_f
$Mg^{2+}_{(AN)} + Fe(phen)_2(CN)_{2\ (AN)} \rightarrow [Fe(phen)_2(CN)_2\cdots Mg]^{2+}_{(AN)}$	−22.1
$2Mg^{2+}_{(AN)} + Fe(phen)_2(CN)_{2(AN)} \rightarrow [Fe(phen)_2(CN)_2\cdots 2Mg]^{4+}_{(AN)}$	−43.0
$2[Mg(H_2O)_6]^{2+}_{(aq)} + Fe(phen)_2(CN)_{2(aq)} \rightarrow [Fe(phen)_2(CN)_2\cdots 2(Mg(H_2O)_5)]^{4+}_{(aq)} + 2H_2O_{(aq)}$	−6.9
$2[Mg(H_2O)_6]^{2+}_{(aq)} + Fe(phen)_2(CN)_{2(aq)} \rightarrow [Fe(phen)_2(CN)_2\cdots 2(Mg(H_2O)_6)]^{4+}_{(aq)}$	−26.0
$[Mg(H_2O)_6]^{2+}_{(aq)} + Fe(phen)_2(CN)_{2(aq)} \rightarrow [Fe(phen)_2(CN)_2\cdots Mg(H_2O)_6]^{2+}_{(aq)}$	−19.7

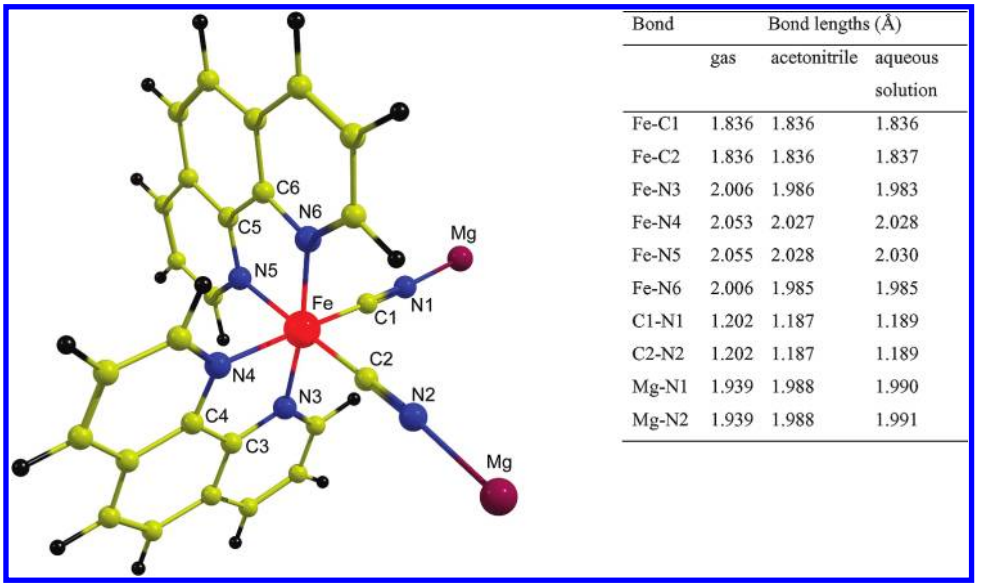

Bond	Bond lengths (Å)		
	gas	acetonitrile	aqueous solution
Fe-C1	1.836	1.836	1.836
Fe-C2	1.836	1.836	1.837
Fe-N3	2.006	1.986	1.983
Fe-N4	2.053	2.027	2.028
Fe-N5	2.055	2.028	2.030
Fe-N6	2.006	1.985	1.985
C1-N1	1.202	1.187	1.189
C2-N2	1.202	1.187	1.189
Mg-N1	1.939	1.988	1.990
Mg-N2	1.939	1.988	1.991

Figure 6. DFT/PBE/CB-1 geometry of $[Fe(phen)_2(CN)_2\cdots 2Mg]^{4+}$ complex in gas phase, acetonitrile, and aqueous solution (global solvation).

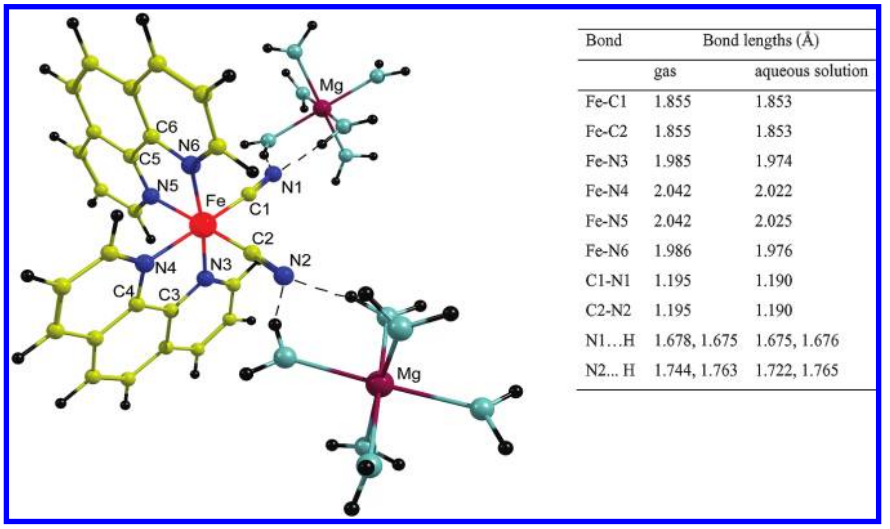

Bond	Bond lengths (Å)	
	gas	aqueous solution
Fe-C1	1.855	1.853
Fe-C2	1.855	1.853
Fe-N3	1.985	1.974
Fe-N4	2.042	2.022
Fe-N5	2.042	2.025
Fe-N6	1.986	1.976
C1-N1	1.195	1.190
C2-N2	1.195	1.190
N1…H	1.678, 1.675	1.675, 1.676
N2... H	1.744, 1.763	1.722, 1.765

Figure 7. DFT/PBE/CB-1 geometry of $[Fe(phen)_2(CN)_2\cdots 2(Mg(H_2O)_6)]^{4+}$ complex in gas phase and aqueous solution.

S4, S5. In acetonitrile, the bonding of Mg^{2+} ions with the cyano N atoms of $Fe(phen)_2(CN)_2$ leads to a shortening of Fe−C bond lengths and slight elongation of Fe−N and C−N bond lengths (Figures 6 and 2). On the other hand, in aqueous solution the effect of the Mg^{2+} ions does not have significant influence on Fe−C, Fe−N, C−N bond lengths, Figures 7 and 3.

To approach the experimental conditions for UV−vis absorption in acetonitrile, we performed TDDFT calculations using the $[Fe(phen)_2(CN)_2\cdots 2Mg]^{4+}$ complex in acetonitrile (Figure 8 at PBE/C-2 level, Supporting Information, Figure S6 at B3LYP/C-2 level). The TDDFT/PBE calculations in acetonitrile predict for $[Fe(phen)_2(CN)_2\cdots 2Mg]^{4+}$ a vertical excitation energy of the most intense absorption band at 2.30 eV (540 nm), which is increased by 0.35 eV (97 nm) compared to $Fe(phen)_2(CN)_2$ (1.95 eV (637 nm)). Hence, in terms of cluster formation of $Fe(phen)_2(CN)_2$ with Mg^{2+} the intense absorption band is calculated to be blue-shifted in line with the observed ionochromic blue shift of the absorption band of Fe^{II} complex.[6] The experimental band maxima of the Fe^{II} complex are located at 597 nm/2.08 eV in pure acetonitrile and at 521 nm/2.38 eV in the presence of Mg^{2+}. The observed ionochromic blue

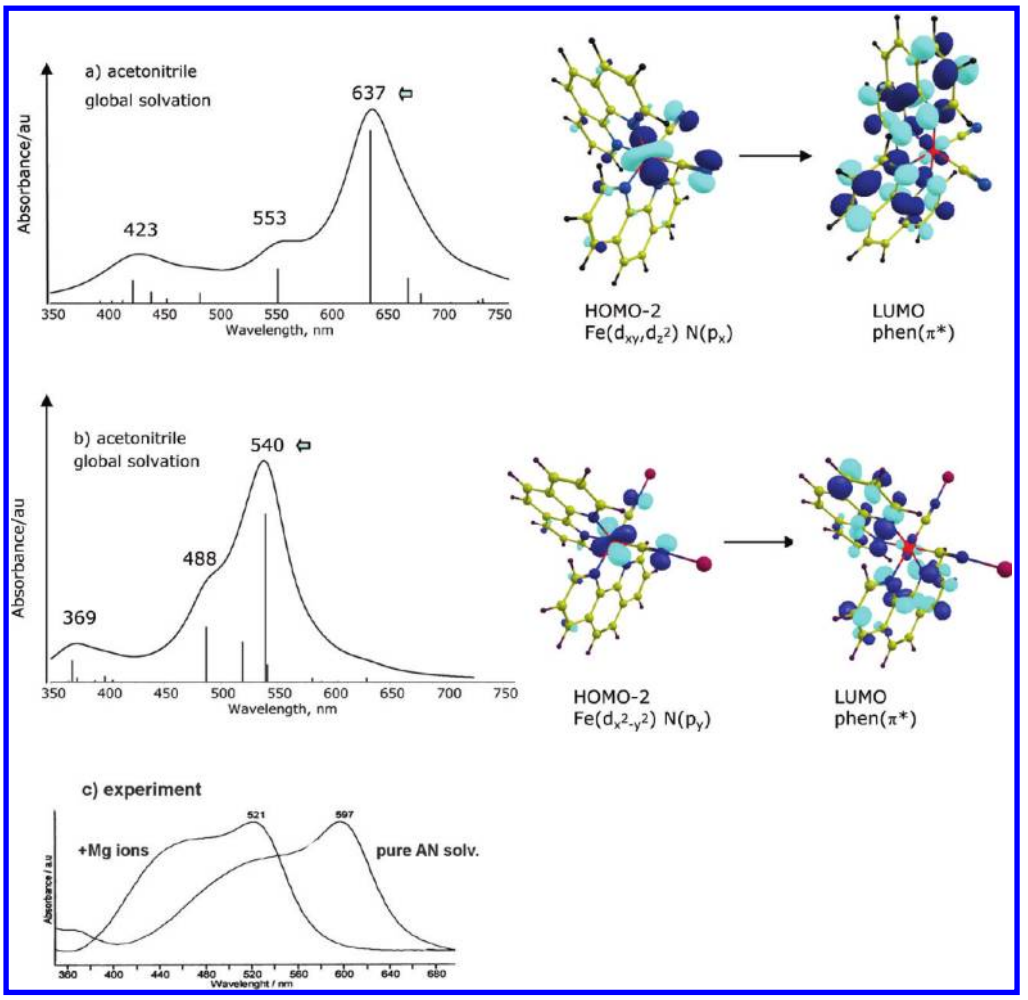

Figure 8. TDDFT/PBE/CB-2 absorption spectra of (a) $Fe(phen)_2(CN)_2$, (b) $Fe(phen)_2(CN)_2\cdots 2Mg]^{4+}$ in acetonitrile, and (c) comparison with the experimental absorption spectra.[6] Plots of orbitals contributing to the most intense transition.

shift (60 nm) of the low intense absorption band[6] was also calculated at the PBE level. The band at 2.24 eV (553 nm) shifts to 2.54 eV (488 nm), Figure 8. The calculated PBE transitions reproduce better the intensity profile of the experimental bands than that at the B3LYP level. As compared to the experimental band maxima, the PBE vertical excitation energies are underestimated by 0.1−0.2 eV whereas those obtained with TDDFT/B3LYP method are overestimated by 0.5−0.7 eV. The B3LYP calculations showed the same trend and blue shift of 79 nm. The shift of 79 nm calculated with TDDFT/B3LYP is more consistent with the experimental value of 76 nm.[6] The plots of orbitals in Figure 8 show the MLCT character of the most intense transition in the $[Fe(phen)_2(CN)_2\cdots 2Mg]^{4+}$ complex. For comparison, the B3LYP and PBE absorption spectra of the two Mg^{2+} clusters, $[Fe(phen)_2(CN)_2\cdots 2Mg]^{4+}$ and $[Fe(phen)_2(CN)_2\cdots Mg]^{2+}$ in acetonitrile are presented in Supporting Information, Figure S7. The cluster with two Mg^{2+} ions shows lower energy transition (~0.1 eV) and a red-shift of ~20 nm as compared to the absorption band of the cluster with one Mg^{2+}.

Inspection of the calculated geometry parameters shows that the Mg^{2+} bonding (in acetonitrile, Figure 6) and the four water molecules bonding to cyano nitrogens (micro+global solvation, Figure 3) produce similar bond length changes in $Fe(phen)_2(CN)_2$, that is, shortening of Fe−C and elongation of C−N and Fe−N bond lengths. These effects are stronger in the case of $[Fe(phen)_2(CN)_2\cdots 2Mg]^{4+}$ formation. Both specific interactions (Fe^{II} complex with water molecules in aqueous solution or with Mg^{2+} in acetonitrile) lead to blue shifts in the absorption bands as compared to that of $Fe(phen)_2(CN)_2$ in acetonitrile, and the shift is larger in the case of Mg^{2+} interaction. Hence, the explanations given for the solvatochromic shift are also valid for the ionochromic shift due to Mg^{2+} ions in acetonitrile. Since both Fe(d) and cyano N(p) orbitals contribute to the occupied orbital of the Fe^{II} complex (included in the most intense transition), the interaction of Mg^{2+} with the cyano nitrogens produces a preferential stabilization of this orbital, causing a higher energy transition and blue band shift. It is expected that the specific interaction with Mg^{2+} ions strengthens the dipole moment and produces ground state stabilization. The CDA calculations predict larger π-back-donation contribution to the $Fe^{II}-CN^-$ bonding upon Mg^{2+} interaction (Table 2) and hence a decrease of the metal electron density. At the same time, a stabilization of the orbital with a main contribution of Fe(d) is suggested to be responsible for the higher energy transition.

To investigate the ionochromic behavior of the iron(II) complex in aqueous solution, the calculated absorption

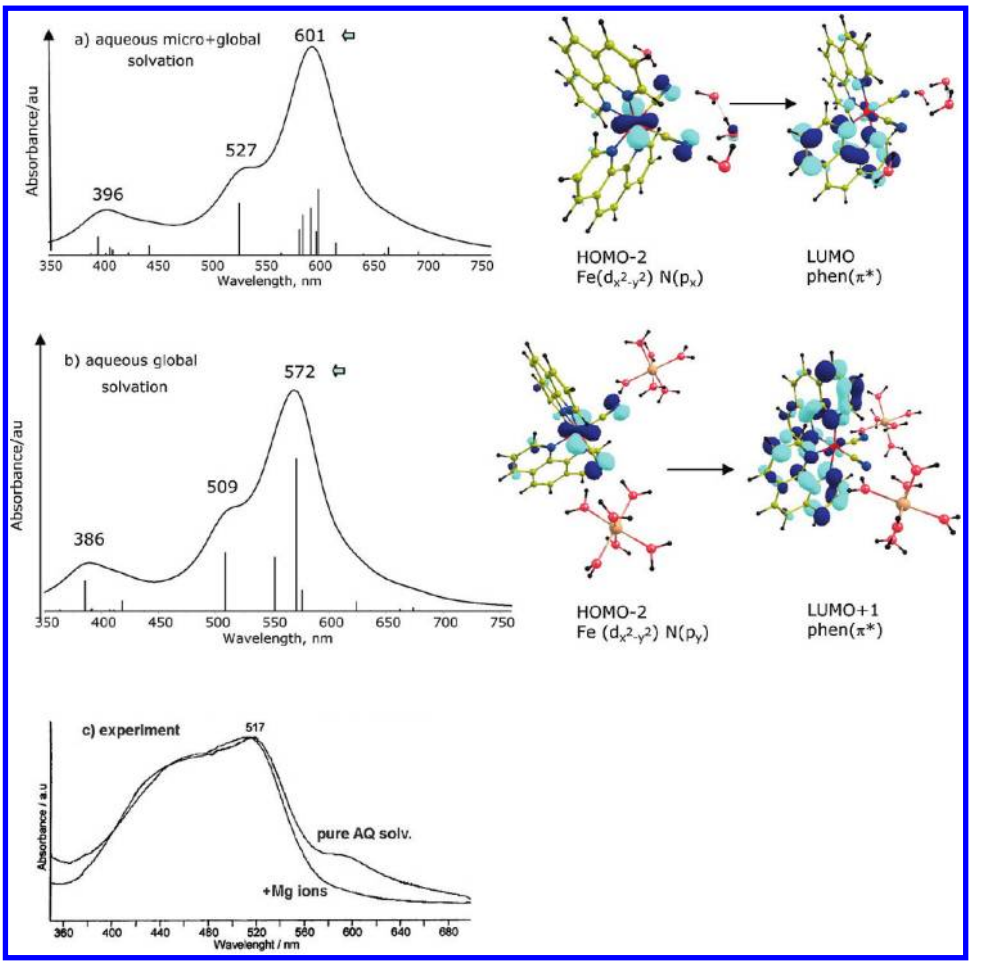

Figure 9. TDDFT/PBE/CB-2 absorption spectra of (a) $Fe(phen)_2(CN)_2\cdots4(H_2O)$, (b) $Fe(phen)_2(CN)_2\cdots2Mg(H_2O)_6]^{4+}$ in aqueous solution (micro + global solvation), and (c) comparison with the experimental absorption spectra.[6] Plots of orbitals contributing to the most intense transition.

spectra of the most stable $[Fe(phen)_2(CN)_2\cdots2Mg(H_2O)_6]^{4+}$ cluster (Figure 9 at PBE level, Supporting Information, Figures S8, S9 at B3LYP level) and of the solvated complex $Fe(phen)_2(CN)_2\cdots4(H_2O)$ are considered. The TDDFT calculations predicted very similar absorption band positions for the Fe^{II} complex with Mg^{2+} and without, namely, 2.06 eV, 601 nm and 2.16 eV, 572 nm at the PBE level (Figure 9) and 2.97 eV, 417 nm and 3.05 eV, 406 nm at the B3LYP level (Supporting Information, Figure S8). The results obtained are in good agreement with the fact that no ionochromic absorption band shifts for $Fe(phen)_2(CN)_2$ in aqueous solution (517 nm, 2.40 eV) as compared to the presence of Mg^{2+} ions (521 nm, 2.38 eV) observed.[6] B3LYP calculations overestimate the vertical excitation energies by ~0.4 eV whereas the PBE calculations underestimate them (by ~0.2 eV). Comparison of the $Fe(phen)_2(CN)_2$ geometry in water (micro and global solvated Fe^{II} complex, Figure 3) and in the presence of Mg^{2+} ions in water solution (cluster of Fe^{II} with Mg^{2+}, Figure 7) show similar bond lengths. Thus, one may conclude that the interactions of hydrated Mg^{2+} and water, respectively, with the cyano nitrogens produce similar geometrical and energetic changes for the ground and the excited states. The most intense absorption bands of the two structures above show the same MLCT character of the transition consisting of mixed Fe(d) and cyano N(p) orbital and phen(π^*) orbital (Figure 9). It should be mentioned that all three clusters of Fe^{II} complex with solvated Mg^{2+} ions, directly bonded to cyano groups (Supporting Information, Figure S4) and bonded through water molecules (Figure 7 and Supporting Information, Figure S5) show similar absorption spectra, Supporting Information, Figure S9. Therefore, the absence of the ionochromic band shift of Mg^{2+} in aqueous solution is not an effect of the Mg^{2+} bonding mode to CN^- groups.

Conclusions

The structural, electronic, and spectroscopic properties of the $Fe(phen)_2(CN)_2$ complex in vacuo, acetonitrile, and aqueous solutions, as well as in presence of Mg^{2+} cations, have been investigated by means of combined DFT/TDDFT methods using B3LYP and PBE functionals. Support by comparison with DFT/MRCI results is given. It has been shown that the overall shape, the band separations, and the solvatochromic absorption band shift of the complex are well reproduced only after consideration of solvent effects both on geometries and on vertical excitation energies. The solvatochromic blue shifts of the two intense absorption bands appearing in the UV−vis spectrum were described by simulating specific solute−solvent interactions and global solvent effects. The global solvation continuum approach for aqueous solution is not sufficient to reproduce the reorganization of the ground and the excited states of $Fe(phen)_2(CN)_2$, that is, the blue band shift as compared to that in acetonitrile.

The TDDFT calculations reproduce the ionochromic blue shifts of both intense absorption bands of $Fe(phen)_2(CN)_2$ upon Mg^{2+} interaction in acetonitrile. The geometrical, electronic, and photophysical properties of the Fe^{II} complex-Mg^{2+} clusters in aqueous solution resemble that of the micro- and global aqueous solvated Fe^{II} complex and, as a result, the ionochromic band shift in aqueous solution is missing.

On the basis of population analysis, the two UV−vis absorption bands of all $Fe(phen)_2(CN)_2$ systems studied are assigned to charge-transfer transitions from hybrid orbitals composed of iron(d) and cyano nitrogen(p) orbitals to phen(π^*) orbitals. The blue band shifts (increasing vertical excitation energies) of $Fe(phen)_2(CN)_2$ going from acetonitrile to aqueous solution or in the presence of Mg^{2+} ions in acetonitrile compared to pure solvent are explained by preferential stabilization of the highest occupied orbitals. The specific interaction of $Fe(phen)_2(CN)_2$ with water solvent molecules and Mg^{2+} ions in solution are responsible for the energy lowering of Fe(d)/cyanoN(p) orbitals, as well as for increasing dipole moment and ground state stabilization. Since the specific interactions of $Fe(phen)_2(CN)_2$ are concentrated on the CN^- groups, they have the decisive role for the observed blue shifts of the UV−vis absorption bands.

Acknowledgment. The work is supported by Bulgarian Science Fund, Grants DO-02-233 and DO-02-82, and by the Austrian Science Fund within the framework of the Special Research Program F16 (Advanced Light Sources) and Project P18411−N19. I.G. acknowledges financial support by the Austrian Academy of Sciences during her stay at the Institute for Theoretical Chemistry, University of Vienna, in the framework of the Bilateral Exchange Agreement Austria−Bulgaria. We thank Professor Peter Schuster for his support of this work. The authors thank Prof. Dr. Stefan Grimme and Prof. Dr. Christel M. Marian for providing the DFT/MRCI program. The calculations were performed in part on the Schrödinger III cluster of the University of Vienna.

Supporting Information Available: Tables S1 and S2 and Figures S1−S9. This material is available free of charge via the Internet at http://pubs.acs.org.